ENERGY LABORATORY

MASSACHUSETTS INSTITUTE
OF TECHNOLOGY

LASER INDUCED DEPOSITION OF THIN FILMS

by

Dr. T. Gattuso, Mr. M. Meunier

and

Dr. J. S. Haggerty

MIT-EL 82-022

ABSTRACT

A new chemical vapor deposition (CVD) process has been demonstrated with Si thin films. In this process, reactant gases are heated by absorbing light energy emitted from an IR laser. No other surfaces are heated by the reaction, thus contamination is eliminated, the state (stress, crystallinity, grain size, etc.) of the film can be controlled and unwanted heterogeneous reaction sites are eliminated.

Research conducted to date has employed silane (SiH_4) as a reactant and an untuned CO_2 laser. Process conditions appropriate for film deposition have been defined. Deposition kinetics, film characteristics and mixed gas optical absorptivities have been measured. Deposition rates are comparable to other low pressure CVD processes (~ 1-10 Å/sec) but with much colder substrate temperatures being permitted. The characteristics of initial amorphous Si films indicate that they equal or exceed the quality of films deposited by highly developed plasma or reactive sputtering techniques.

TABLE OF CONTENTS

LIST OF FIGURES

LIST OF FIGURES (cont.)

I. INTRODUCTION AND BACKGROUND

For several years we have studied the synthesis of ceramic powders by means of laser heated gas phase reactions.[1] In these processes, reactant gases are heated by absorbing light emitted from an infrared laser much as moisture is heated by microwave energy. The unusual process characteristics that can be achieved readily with laser heating have permitted us to produce nearly ideal powders of Si, Si_3N_4 and SiC with excellent energy and mass utilization efficiencies. Over 95% of the reactant gases are converted in a single pass through the laser beam with approximately 2 kWhr of heat per kilogram of powder.

The powder synthesis process is well modelled at this time. We understand how to manipulate process variables to produce extremely uniform, small diameter, agglomerate free, high purity powders. This modelling has lead us to the conclusion that laser driven reactions can be applied to a wide range of chemistries in which either homogeneous gas phase nucleation or heterogeneous nucleation on substrates can be controlled precisely. Recently, we have begun to develop a laser heated chemical vapor deposition (CVD) process that appears widely applicable to electronic, optical and corrosion protection applications. We have successfully deposited amorphous silicon onto a variety of substrates by means of laser-induced pyrolysis of silane gas. We feel that the laser heated CVD process represents an extremely exciting opportunity at this time.

In the CVD process, laser intensity, gas optical absorptivity, gas pressure and system geometry are manipulated to cause heterogeneous

nucleation on a substrate surface, rather than homogeneous nucleation of particulate reaction products. The laser heated CVD process has many unique characteristics. It is possible, for example, to set the gas and substrate temperatures independently. It is not necessary to heat the substrate to the reaction temperature and this is expected to be an advantage over conventional pyrolysis processes (e.g. Si on sapphire). Reduced substrate temperatures: 1) reduce stresses that result from mismatches between film and substrate thermal expansion coefficients; 2) permit a wider range of deposited material and substrate combinations; 3) allow control of the crystalline state of the film; and 4) reduce contamination and problems of interaction between film and substrate. The reduced substrate temperature should permit the use of low cost, low temperature, plastic or glass substrates with pyrolysis reactions that occur only at high temperatures. The location of the reaction can be positioned at any arbitrary point above the substrate by means of intersecting beams. Extremely high purities, good energy efficiencies and complete utilization of reactant gases are all achievable based on the results of the powder synthesis process research.

Our initial research efforts have explored the applicability of this CVD process for producing silicon containing films. It is apparent that the process can be applied to other materials; we have selected silicon chemistries as the initial research vehicle for studying this process because we already have measured the optical characteristics of SiH_4 gas and there is such an enormous market for Si, as well as related SiO_2 and Si_3N_4 films, in various electronics applications.

Over the past seven years, there has been growing interest in a class of amorphous semiconductors deposited in thin film form in the presence of hydrogen.[2] The interest is derived primarily from certain electronic properties that make the materials potential candidates for solar photovoltaic energy conversion[3] and thin film device applications. The unusual properties of a-Si:H are associated with the fact that it contains between 5 to 30 at. % hydrogen, which saturates dangling bonds leading to the ability to control the Fermi level by substitutional doping. This material is usually produced by glow-discharge decomposition of silane[4] and reactive sputtering in hydrogen[5]. CVD also has been used to give good quality amorphous films, but due to the high substrate temperature (T_s ~ 600°C) necessitated by the kinetics of film deposition, less than 1 at. % H is present in the material. This is not enough hydrogen to achieve good electronic properties.[6] In the laser CVD process, high deposition rates can be achieved at low T_s, leading to films containing adequate hydrogen.

II. LASER-INDUCED PYROLYSIS OF SILANE

A. Introduction

This process is distinctly different from other semiconductor processing operations that employ lasers. Two of the most widely studied and cited laser processes involve laser annealing of damage after ion implantation,[7] and inducing localized pyrolysis reactions[8-10] by laser-heating of substrates. In the process described here the reactant gases are heated directly by absorbing light emitted from a laser, consequently the reaction

zone can be extremely uniform and precisely controlled. In addition, the laser beam does not provide a surface that dominates various heterogeneous nucleation and reaction effects.

Christensen and Lakin[8] observed enhanced deposition rates of silicon from silane in laser-heated substrate experiments when wavelengths were used that were absorbed by the gas as well as by the substrate. Bilenchi and Musci[11] recently reported similar observations, and also have succeeded in depositing amorphous silicon onto substrates by a technique very similar to the one described in this report. The geometry of the deposition system of Boyer et al.[12] is nearly identical to that of the system used in this work; however their use of uv light results in a different sort of photochemical process from the one described below. Finally, Deutsch et al.[13] report deposition of metal films with microscopic features by means of uv laser-induced photochemical decomposition of gases.

B. Optical Absorption

The optical absorption coefficients (α) of the reactant gases determine the fraction of the incident laser power absorbed by the gas. This determines heating rates and the overall efficiency of the process, so that ultimately the accuracy with which the deposition process can be modeled depends on how precisely α is known. The effective absorption coefficient is a function of the overlap between the absorption spectrum of the reactant gases and the emission spectrum of the laser. Since the untuned high power CO_2 lasers emit almost totally at the P(20) line at 10.591 μm (944.195 cm^{-1}), it is α at this wavelength that is most important.

The low pressure absorption spectra of gases such as silane are made up of many narrow absorption lines spaced at somewhat regular intervals. Since it is highly unlikely that a single absorption line will have exactly the same wavelength as an emission line of the laser, the difference between the positions of the two lines and their respective line widths will determine α. At low pressures (< 1 torr), Doppler broadening determines the width of the absorption line. The Doppler width, $\Delta\nu_D$, can be calculated from:[14]

$$\Delta\nu_D = 7.16 \times 10^{-7} \left(\frac{T}{M}\right)^{1/2} \nu_o \qquad (cm^{-1}) \qquad (1)$$

where T is the temperature, M the molecular weight, and ν_o the line center in cm^{-1}. The absorption coefficient at position ν is equal to:[14]

$$\alpha_\nu = \alpha_o \exp - \left[\frac{2(\nu-\nu_o)(\ell n 2)^{1/2}}{\Delta\nu_D}\right]^2 \qquad (2)$$

where α_o is the coefficient at the line center. As the line broadens with increasing temperature, α_o decreases such that the integrated absorption, S, remains constant:

$$S = \int \alpha_\nu d\nu = \left(\frac{\pi}{\ell n\ 2}\right)^{1/2} \left(\frac{\Delta\nu_D}{2}\right)\alpha_o = \text{constant} \qquad (3)$$

The absorbtivity is very small if the absorption and emission lines are more than a few Doppler widths apart. As an example, the SiH_4 absorption line nearest the P(20) CO_2 line[15] is at 944.213 cm^{-1}, thus the positional difference is only 0.018 cm^{-1}. The calculated Doppler widths of this absorption line are 2.1 x 10^{-3} cm^{-1} at 300K and 4.6 x 10^{-3} cm^{-1} at 1500K, with the resulting values of α_ν being about 10^{-91} α_o and 10^{-18} α_o, respectively. From these values, it is obvious that for silane at low pressures, any absorption will be an artifact due to rare isotopes of silicon in the silane or forbidden energy transitions.

At system pressures above a few torr, collisions between the gas molecules cause the absorption line widths to broaden. For many gases, this broadening, $\Delta\nu_L$, has been found empirically to be proportional to the system pressure:[14]

$$\Delta\nu_L = kP \tag{4}$$

In the presence of pressure broadening, and when $\Delta\nu_L >> \Delta\nu_D$, the absorptivity can be approximated by:[14]

$$\alpha_\nu = \left[\alpha_o\left(\frac{1}{\pi \ell n 2}\right)^{1/2} \frac{\Delta\nu_D}{\Delta\nu_L}\right] \left[\frac{1}{1 + \left(\frac{2(\nu - \nu_o)}{\Delta\nu_L}\right)^2}\right] \tag{5}$$

The first term in brackets is the absorption at the peak; it is inversely proportional to pressure. When $(\nu - \nu_o) = \Delta\nu_L/2$, the absorptivity at

position ν has its maximum value:

$$\alpha_{max} = \frac{\alpha_o}{4}\left(\frac{1}{\pi \ln 2}\right)^{1/2} \frac{\nu_D}{(\nu - \nu_o)} \qquad (6)$$

In the case of silane and for 10.6μm, $\alpha_{max} = 0.01\ \alpha_o$ at 300K according to Equation 6.

The intense laser radiation can change the absorptivity of the gas. At room temperature virtually all of the gas molecules are in the ground vibrational level, and they are distributed among approximately twenty rotational levels according to a Boltzmann distribution. As the gas is heated, some rotational levels experience an increase in population, and others experience a loss. Since only one rotational level of the ground vibrational level absorbs the laser radiation, changes in the gas temperatures will change the number of molecules that are capable of absorbing the monochromatic light. Although the exact rotational quantum number of the absorbing level in silane is not known, it is apparently higher than the room temperature average. An increase in temperature will therefore increase the silane absorptivity.

Whenever an infrared photon is absorbed, a molecule makes a transition to an excited vibrational level. Collisions soon return this molecule to the ground state, but in the mean time it is unable to absorb another photon unless a transition between the first and second excited vibrational levels is also resonant with the 10.6 μm radiation. Since the spacing between excited vibrational levels in silane is unknown, it is impossible to predict

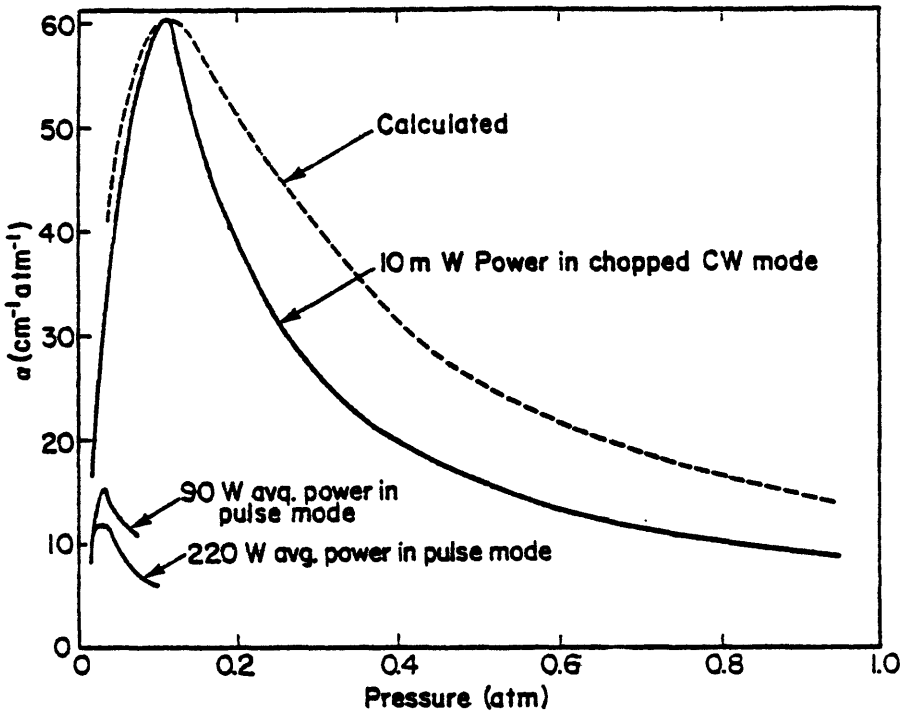

Figure 1. The absorption coefficient of SiH_4 as a function of pressure for the P(20) CO_2 laser line (Reference 1).

whether a large degree of vibrational excitation will increase or decrease the absorptivity of silane. This will have to be experimentally determined. Figure 1 shows the optical absorptivity of silane as a function of gas pressure and laser intensity.[1] These data show that α_{SiH_4} is strongly dependent on pressure and laser intensity, perhaps as a temperature effect.

The strong dependence on pressure is expected based on Equation 5 for α_ν. A curve for α_ν calculated from Equation 5 using the experimental peak of $\alpha_{SiH_4} = 60\ (atm \cdot cm)^{-1}$ at 85 torr is also included in Figure 1. Agreement between the experimental and calculated absorptivities is good up to the peak, but the experimental absorptivity falls off more rapidly than expected. This may be due to a small amount of non-P(20) emission from the laser that is not absorbed by the silane. If so, a repeat of the low intensity measurement with a still shorter cell will reveal the true high pressure absorption.

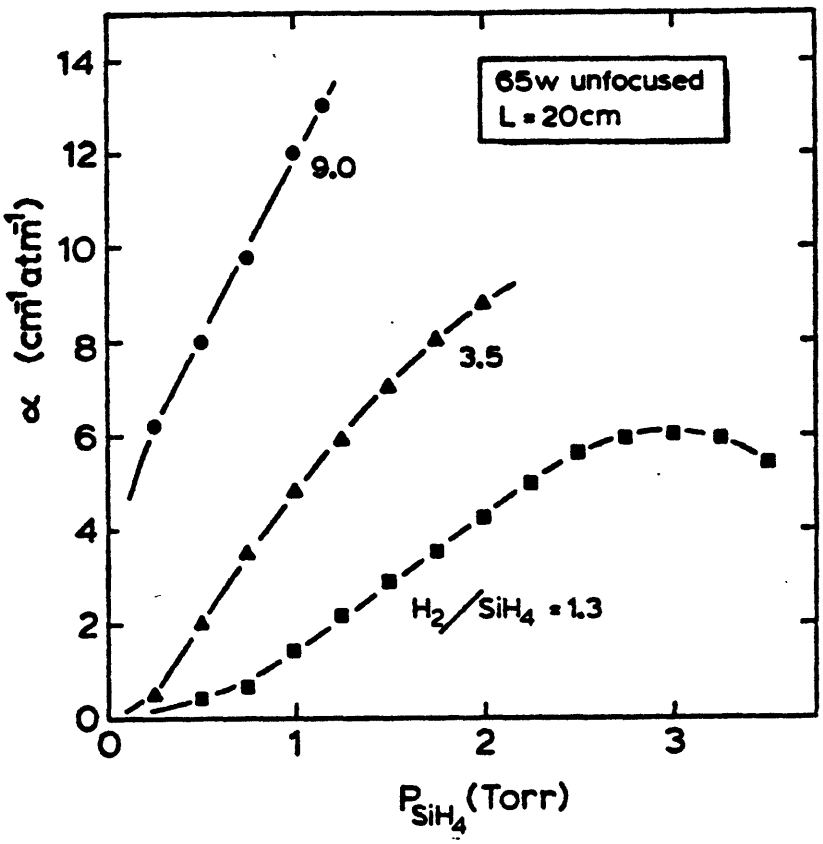

Figure 2. The absorption coefficient of SiH_4 as a function of silane partial pressure and the hydrogen to silane ratio for the P(20) CO_2 laser line.

Absorption line broadening also results from collisions with foreign gas molecules, or Lorentz broadening, in contrast to the pressure dependence displayed in Figure 1 that results from collisions of silane molecules with other silane molecules. Lorentz broadening is due to the temporary formation of a quasi-molecule between an absorbing molecule and a foreign molecule.[16] The broadening is explained by transitions that occur between the two potential energy curves of the quasi-molecule. Figure 2 shows the dramatic effect of hydrogen, which is transparent, on silane absorptivity. At a silane partial pressure of 1 Torr the absorptivity increases by an order of magnitude as the H_2:SiH_4 ratio is increased from 1.3 to 9. The maximum in the data for the highest hydrogen concentration is not a real pressure broadening maximum and suggests the onset of some sort of saturation.

C. Silane Photochemistry

The overall chemical reaction of interest in this research is:

$$SiH_4(g) \rightarrow Si(s) + 2H_2(g) \ . \qquad (7)$$

For the formation of crystalline silicon the reaction is exothermic with $|\Delta H| \approx 5\text{-}6$ kcal/mole. The reaction is still exothermic if amorphous Si is produced, and the magnitude of ΔH is reduced by a few hundred cal/mole.

Photons from the CO_2 laser light do not interact with silane to form silicon according to Equation (7) in a single absorption event. The energy of a 10.6 μm wavelength photon is only about 1/10 eV, while energies an order of magnitude higher are required to break chemical bonds. When an infrared photon is absorbed the absorbing molecule makes a transition to an excited vibrational level. Collisions distribute the absorbed energy and return the absorbing molecule to the ground state, but in the mean time it is unable to absorb another photon. The overall effect is an increase in temperature. Deutsch[17] found no evidence for multiphoton, collisionless processes in silane at CO_2 P(20) fluences up to 150 J/cm^2. CO_2 laser pyrolysis of silane is essentially a thermal process and therefore collisions are extremely important.

Intermolecular collisiona are required for the distribution of absorbed energy. In this kind of process, if one of a mixture of gases absorbs, the entire mixture is heated. This has important consequences concerning the deposition of compounds. Collisions also are required to improve coupling between the absorber and the radiation. Too many collisions in the gas phase result in particle nucleation, and the dependence on collisions precludes spectroscopic selectivity of reaction paths.

The precise mechanism for the thermal decomposition of silane is not known. Deutsch[17] observed molecular hydrogen lines in the luminescence of silane excited by high energy CO_2 laser pulses. Mass spectroscopic analyses gave no evidence of Si_2H_6, and it was concluded that the dominant initial dissociation step is:

$$SiH_4(g) \rightarrow SiH_2(g) + H_2(g) \qquad (8)$$

Bilenchi and Musci[11] concluded from mass spectroscopic evidence that dissociation occurs in the gas phase in CO_2 laser-induced pyrolysis of silane. They observed SiH_2, SiH_3 and molecular hydrogen in the product vapor. They also observed only weak dependence of deposition rate on substrate temperature. Scott et al.[18] concluded from deposition rate measurements that $SiH_2(g)$ is the precursor of amorphous silicon films produced in so-called homogeneous chemical vapor deposition of silicon from silane. In that process a cooled substrate is placed in a hot-walled reactor. The dependence of deposition rate on substrate temperature observed by Scott et al.[18] agreed, at least qualitatively, with that predicted by Sladek[19] in his general model for homogeneous CVD. Scott et al.[18] hypothesize rapid surface reactions as responsible for the reduction in the H:Si ratio in deposited films. In studies of mercury-sensitized photolysis of SiH_4, formation of Si_2H_6 and Si_3H_8, as well as H_2, has been reported,[20] although high energy uv photons are employed in this process and one might expect a different reaction path from that in a thermal process.

III. DEPOSITION EXPERIMENTS

A. Deposition System

The apparatus that was used in the initial work is shown in Figure 3. Substrates are mounted on a temperature controlled stage* in a brass reaction cell; substrate temperature is monitored by means of a thermocouple in contact with the stage. Although substrate heating is not necessary for deposition to occur, the substrate temperature is expected to have a significant effect on the properties of the resultant films and is expected to be an important variable in process optimization. Generally, substrate temperatures have been in the 250 to 350°C range for these experiments.

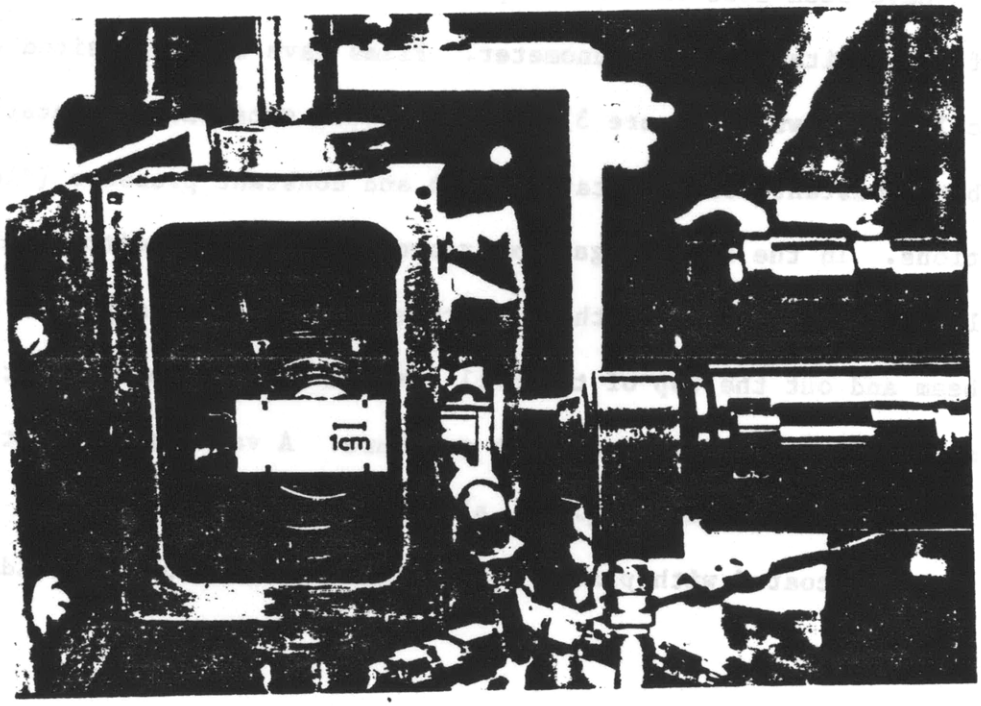

Figure 3. Reaction cell with heated substrate stage used in the laser CVD experiments.

* NTK Technical Ceramics

Infrared radiation is supplied by a Coherent Radiation Everlase 150 untuned CO_2 laser operated in cw mode. The cell is fitted with potassium chloride windows. The axis of the laser beam is made to pass through the cell, parallel to the substrate plane at a distance of approximately one beam diameter. The unfocused beam diameter is 6 mm; a lens with a focal length of 12.7 cm was used in the experiments involving a focussed beam. A thermopile was used to monitor the laser power transmitted through the cell. Incident laser energy densities have been in the 100 to 1000 watts/cm^2 range.

Pure silane,* typically at pressures of 4 to 7 Torr, has been used in most of the experiments so far. Mixtures of silane and helium, and of silane and hydrogen have been used in a few experiments. Cell pressure is monitored by means of a capacitance guage manometer. Films have been deposited with both vertical (as shown in Figure 3) and horizontal substrate orientations, and under both constant volume (static cell) and constant pressure (flowing gas) conditions. In the flowing gas experiments silane is admitted through a 1 mm ID cylindrical nozzle below the substrate stage. The gas passes through the laser beam and out the top of the cell through a filter and throttling valve assembly that maintains a constant pressure. A variety of substrate materials including borosilicate glass, aluminum, aluminum oxide and borosilicate glass coated with platinum, molybdenum or indium-tin oxide has been used.

---

*Airco Grade 3

Deposition rate measurements were made with an interferometric technique shown schematically in Figure 4. Light from a He-Ne laser (λ = 6328 Å) is shined on the substrate at near normal incidence. The intensity of the reflection is monitored by means of an appropriately filtered silicon photodiode. In these experiments the back surfaces of the transparent substrates were etched with dilute HF so that only the front surface reflections were recorded. As the film thickness increases, the reflectance passes alternately through maxima and minima as the conditions for constructive and destructive interference, respectively, alternately are satisfied. The conditions for R_{max} and R_{min} are shown in Figure 5.

B. Static Cell Experiments

The overall reaction represented in Equation 7 shows that two moles of gas are produced for each mole of reactant gas that is consumed. Therefore in a constant volume system the pressure should increase as the reaction proceeds. Our initial experiments were of this kind, in which the cell first was evacuated, then filled to some low pressure of silane and then sealed off. At this point the laser beam was made to pass through the cell. Figure 6 shows a typical record of cell pressure and substrate temperature versus time in this kind of experiment. The discontinuities in pressure at the opening and closing of the beam shutter are due to the extremely fast heating of the gas in the beam path when irradiated and the rapid cooling of the gas in the beam path when exposure is terminated. The smooth increase in P during exposure results, in part, from the increase in the number of moles of gas because of reaction and, in part, because of the increase in the

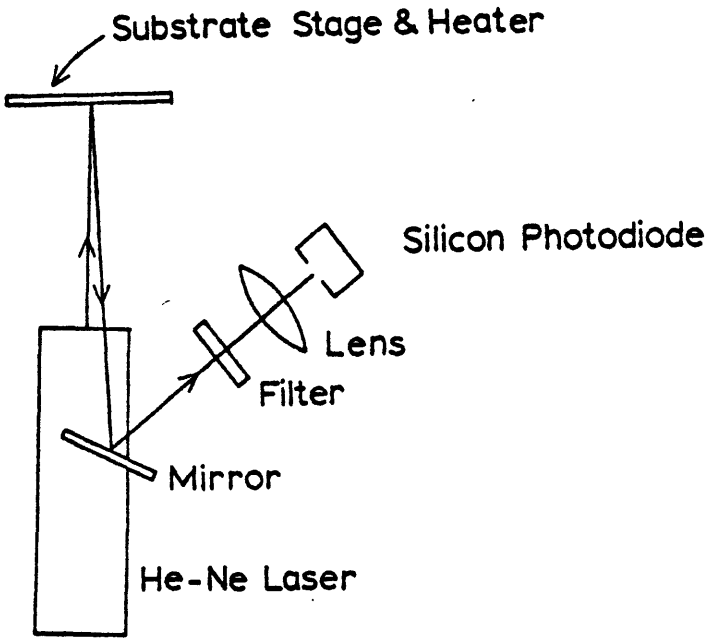

Figure 4. Schematic of the interferometric deposition rate monitoring system.

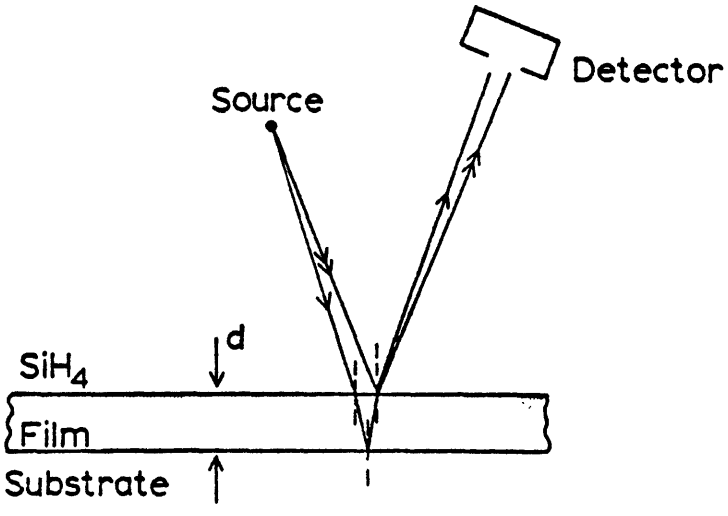

Maxima:

$$d = \frac{(m+0.5)\lambda}{2n}$$

Minima:

$$d = \frac{m\lambda}{2n}$$

m = integer

Figure 5. Conditions for reflectance maxima and minima for a transparent film with index of refraction n.

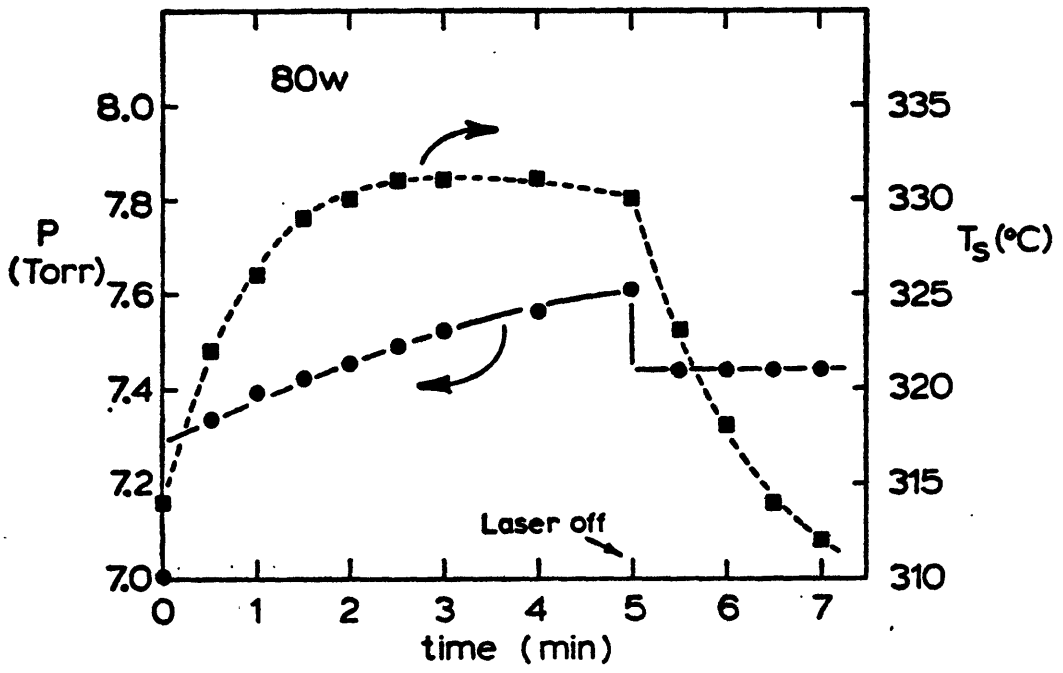

Figure 6. Cell pressure and substrate temperature versus time during a static cell deposition.

average temperature of the system - this latter fact also accounts for the difference in magnitudes of the discontinuous pressure changes. dP/dt decreases with time during deposition; a corresponding decrease in deposition rate with time is observed during static cell experiments. The increase in T_s results, in part, from thermally excited molecules impinging on the substrate and, in part, from the heat released in the pyrolysis reaction at the substrate surface. Notice that T_s passes through a broad maximum.

Qualitatively, the decreases in dP/dt and deposition rate during deposition make sense in terms of the depletion of reactant gas. Mass balance analyses, however, show that in these experiments only about 1% of

the available silane is converted to silicon. It is not expected that changes in concentration of this magnitude significantly lower either the thermodynamic driving force for decomposition because of hydrogen production (see Section V), or the absorptivity. Indeed, one might expect the absorptivity initially to increase because of pressure broadening. The strong dependence of deposition rate on flow rate observed in the constant pressure experiments described below suggests the importance of mass flow in this process. For deposition to continue in the static system once the reaction has begun, fresh silane must diffuse into the beam path. The sharp temperature gradient characteristic of laser heating opposes this diffusion[21] and hinders deposition. We have begun an analysis of the mass flow issues associated with the laser CVD process in an effort to elucidate the time dependence of the deposition rate.

Figure 7 shows a deposited film illuminated at near normal incidence with sodium vapor light. The film was deposited in a static cell experiment in four exposures of 10-15 minutes each. The cell was evacuated and fresh silane was introduced before each exposure. The laser power was 80W; the initial silane pressure and substrate temperature were 7 Torr and 315°C, respectively. The light and dark fringes result from the interference effects described in Figure 5 and represent lines of constant thickness. This deposit was made with a focussed beam; the location of the focus was above point A, which coincided with the center of mass of the substrate stage. It was expected that reaction rates, and therefore deposition rates would be highest at the highest laser intensities. In the focussed beam experiments, however, deposition invariably was observed to occur near the

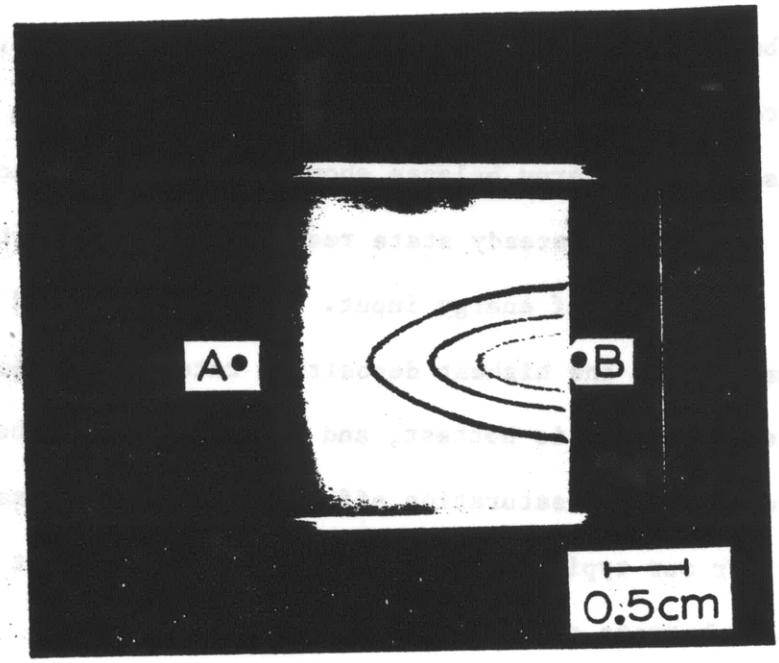

Figure 7. A film of amorphous silicon on a borosilicate glass substrate in reflected monochromatic light. Laser beam propagation direction was from B to A.

entrance end of the cell, well away from the focus. The deposit in Figure 7 nucleated at point B and then grew both normal to and parallel to the beam axis. The center of mass of deposits could be moved toward the center of the substrate stage by moving the beam focus toward the exit end of the reaction cell. In films produced with unfocussed beams the centers of mass of the deposits were observed to coincide with the center of mass of the stage. In the unfocussed beam experiments the laser intensity above the deposit center typically was a factor of 5 to 6 lower than the intensity at the corresponding point in the focussed beam work. There are at least two important considerations here: the effect of the substrate heater and the effect of laser intensity on the absorptivity. The data in Figure 1 show the apparent decrease in α with increasing laser intensity. The effect could be

mass flow related (one expects steeper temperature gradients with higher intensity beams), or some sort of spectroscopic saturation[17] might be occurring. The substrate heater heats the silane in its vicinity, and this is expected to increase the absorptivity, as described in Section IIB. A simple analysis based on an energy balance shows that a hot surface near the laser beam results in a higher steady state reaction zone temperature than a cold surface for a given rate of energy input. For an unfocussed beam these last two effects imply that the highest deposition rates should occur near the substrate center, where it is hottest, and that is what is observed. For a focussed beam, substrate and saturation effects compete. The saturation effect is stronger for our typical conditions, leading to highest reaction rates away from the substrate center.

Substrate effects probably also account for the short deposit dimensions parallel to the beam axis. Again, mass balances show that only a small amount of the available silane is consumed in these experiments. Similarly, only a small fraction of the available laser energy is absorbed in the path above the substrate stage (only about 20%) of the beam is absorbed over the entire 20 cm cell length). Based on these data one would espect the lines of constant thickness to lie parallel to the beam axis over the entire substrate length. Clearly some sort of mapping of the reaction zone, possibly by means of Schlieren photography or an interferometric technique, is required.

At the low pressures employed in the CVD work, gas phase diffusivities are high, accounting for the large deposit dimensions - several beam diameters - normal to the laser beam axis. The low pressures also reduce the effects of convection, and this accounts for the symmetry with respect to the

laser beam of deposits made with vertical substrates. A schematic of the deposition system looking along the beam axis is shown in Figure 8 (approximately to scale). Here X_C represents the distance the center of mass of the irradiated volume rises from the rest due to bouyancy forces, and X_D represents the radial distance an excited molecule diffuses. A comparison of X_C and X_D is shown in Figure 9 for the case of infinite heating rate to an assumed reaction zone temperature of 800°K. Tabulated heat capacity data and our measured absorption coefficients show $\dot{T} \approx 10^6$°C/sec, so the assumption of $\dot{T} = \infty$ is not unreasonable. This comparison very clearly shows that diffusion is the dominant transport mechanism. The calculation is conservative in that thermal gradient effects have been ignored.

The minimal effect of convection, coupled with the very high heating rates attainable with laser heating, allow uniform heating of large sheets of reactant gas by sweeping the laser beam through the gas in a plane parallel to a substrate surface. Production of large areas with uniform deposition will be possible. Laser CVD is expected to have many of the advantages of conventional low pressure CVD[22] without requiring high substrate temperatures.

C. Flowing Gas Experiments

Static cell measurements were useful in determining appropriate process conditions and geometries for film deposition. To study the effects of process variables on the steady state reaction, flowing gas experiments were performed. In these experiments the silane flow rate and cell pressure were established and then the laser beam was made to pass through the cell.

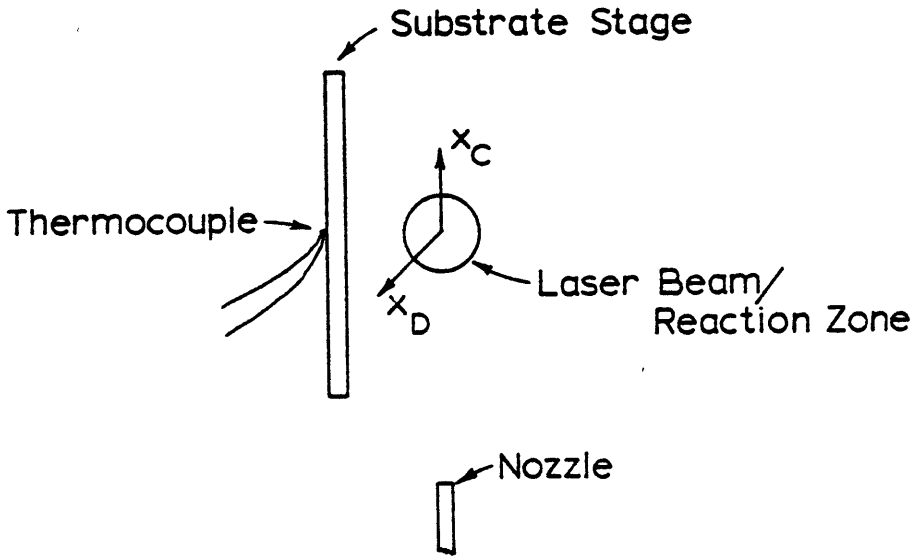

Figure 8. Schematic of the laser CVD system looking along the laser beam.

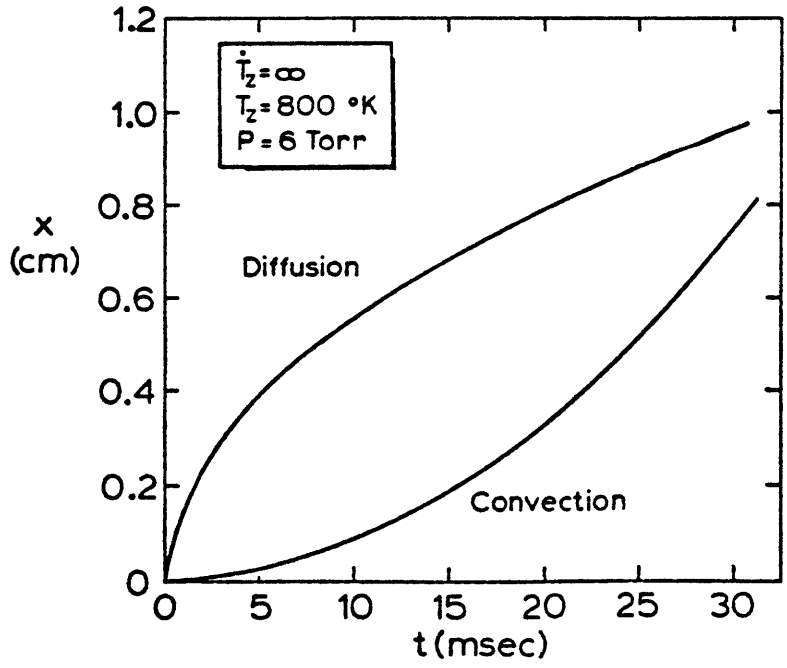

Figure 9. Comparison of convective and diffusional transport mechanisms for an infinite heating rate.

Pressure pulses similar to those shown in Figure 6 were observed upon opening and closing the beam shutter. Deposit locations and sizes did not change compared to static cell work. Figure 10 shows a record of reflectance versus time during deposition in a flowing gas system. The origin of the maxima and minima has been described; the attenuation of the peaks is caused by absorption of the component of the reflected signal that must traverse the film thickness. Absorption limits film thickness measurements to about 0.75 μm with this wavelength light. The range can be extended by using a longer wavelength.

Figure 11 shows a plot of thickness versus time constructed from the positions of the maxima and minima of the reflectance versus time record in Figure 10. The value for the index of refraction at the He-Ne laser wavelength, n = 4.6, was taken from the literature.[23] Thicknesses determined from fringe counting using this value for n agree well with a limited number of independent thickness measurements made with a Sloan Dektak[24] profilometer. Figure 12 shows the instantaneous deposition rate versus time derived from Figure 11. The general shapes of Figures 11 and 12 are typical. It is surprizing that such a long time is required to reach steady state since the substrate should not be a factor at film thicknesses greater than a few hundred angstroms. The average system temperature does increase during deposition and this could be responsible for the long transient. Another possibility is the gradual elimination of impurities, most likely oxygen, as the reaction proceeds.

The maximum deposition rate measured by this technique is about 160 Å/min, although higher rates have been achieved. This compares very well

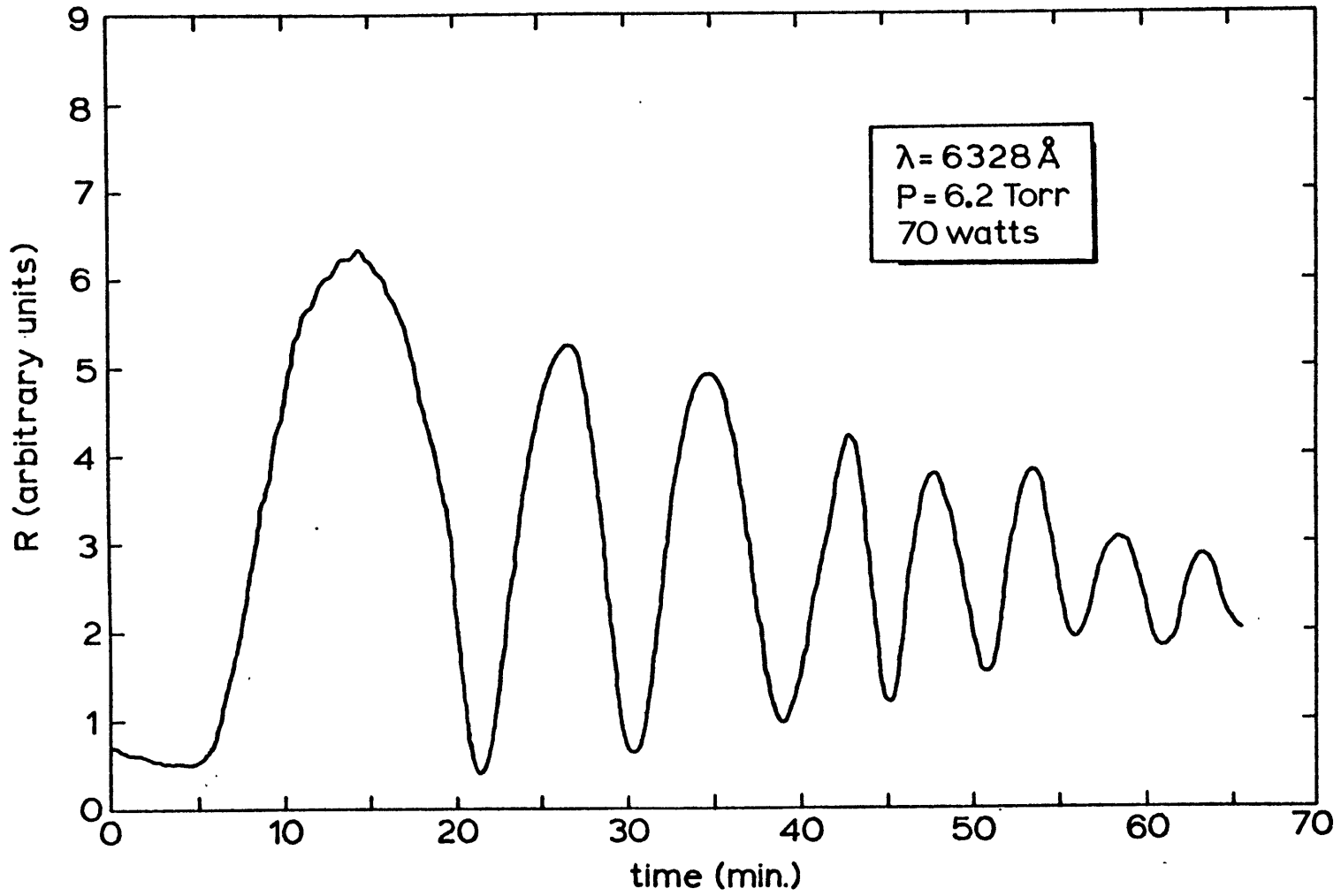

Figure 10. Reflected intensity versus time for a film deposited in a flowing gas experiment.

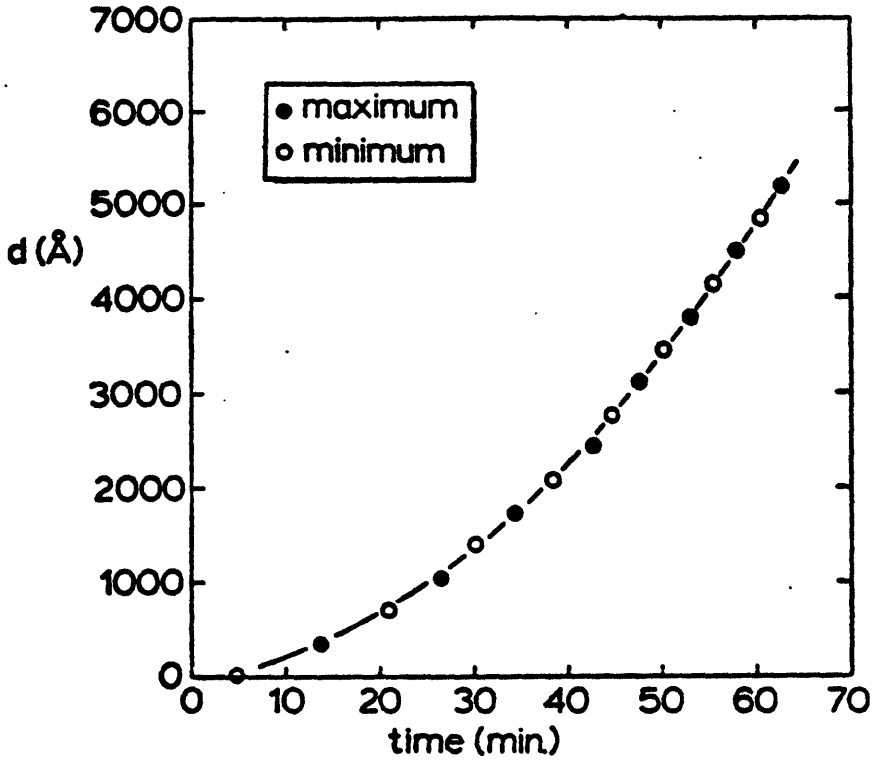

Figure 11. Plot of thickness versus time constructed from the extrema in Figure 10 assuming n = 4.6 (Reference 22).

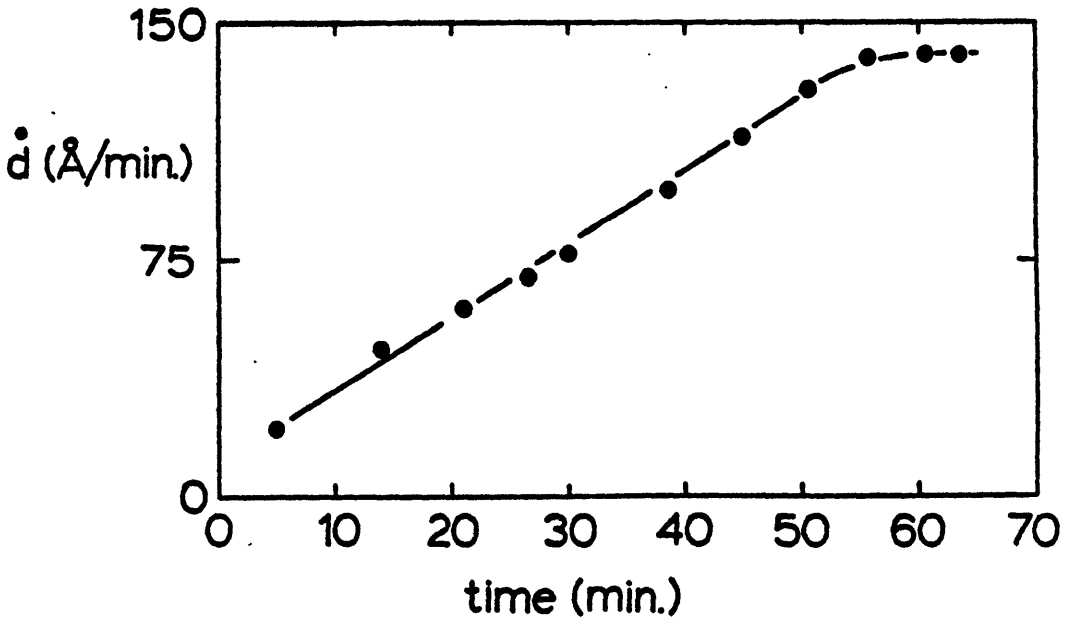

Figure 12. Instantaneous deposition rate versus time constructed from Figure 11.

with deposition rates for a-Si in normal CVD.[25] In normal CVD, where silane gas is passed over heated substrates, deposition rates for a-Si are limited by the onset of crystallinity in the deposit as the substrate temperature is increased. In addition, the amount of retained hydrogen decreases as T_s is increased, resulting in degradation of elecrical properties. In the laser CVD process high deposition rates can be achieved at low T_s, thus eliminating the need for post-deposition hydrogenation.

The deposition rate in the flowing gas experiments was found to depend quite strongly on the silane flow rate, as shown in Figure 13. Under normal constant pressure conditions only about 1% of the silane is consumed in a single pass through the cell, so this effect is not associated with depletion of the total available reactant but rather with getting the reactant into the beam path. It was mentioned above that the steep temperature gradients characteristic of laser heating oppose diffusion of gas molecules into the beam.[21] In the flowing gas system (see Figure 8) fresh silane is forced into the beam. Assuming reaction is rapid once the reactant gas is irradiated a strong dependence of deposition rate on flow rate, which now represents the rate at which reactant is delivered to the reaction zone, should be expected. This means that flow rates must be controlled very precisely if the effects of other process variables on deposition rate are to be observed.

Qualitatively, deposition rates in the laser CVD process increase with increasing substrate temperatures, laser power and silane pressure. The maximum rate is limited by the onset of powder production. It is expected that the range of film production can be extended by using mixtures of silane and either H_2 or HCl to suppress the onset of homogeneous reactions. The

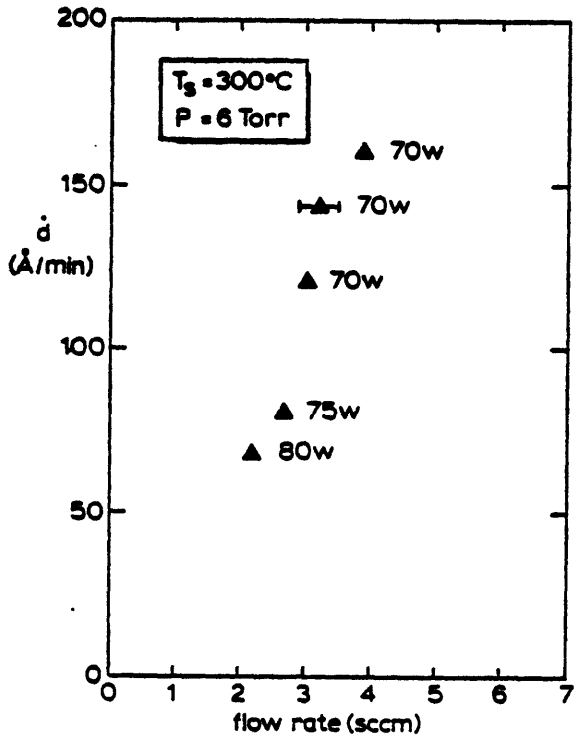

Figure 13. Steady state deposition rate versus silane flow rate for constant substrate temperature, cell pressure and laser power (approximately).

thickest film produced so far is 2 μm thick. This deposit was produced in a static cell experiment and its thickness was measured with a Dektak profilometer.

IV. FILM CHARACTERIZATION

A. Structure

No attempt has been made yet to thoroughly characterize the structure of the films produced by the laser CVD process. Films produced under the conditions described above have been determined to be amorphous by electron

diffraction. This was expected based on the low substrate temperatures used. At no time has any deposit been produced without the laser beam being on.

With clean substrates film adhesion was found to be very good. Occasionally a deposit would peal and curl, indicating a state of tensile stress in the film. In almost all of these cases the origin of the pealing could be traced to contamination (generally particles) on the substrate surface. Pealing of films back from substrate edges also was observed.

B. Electrical and Optical Properties

Some electrical and optical properties of laser CVD a-Si films have been investigated. Preliminary results indicate that the electronic properties are at least as good as those for films produced by glow-discharge and reactive sputtering techniques. These points are highly encouraging in that they were obtained without on optimization. We can expect that further research will improve those properties.

One of the most important criteria for determining the quality of a film is the concentration of defects,[26] which can be evaluated by Electron Spin Resonance (ESR). We have measured a spin concentration $N_s \approx 10^{17}$spins/cm^3 in one of our films deposited at $T_s = 350°C$. This is very encouraging because this value is a factor of 100 lower than N_s of normal CVD films[6] and is the same order of magnitude as that of high quality films produced by glow-discharge.[2,4] This result indicates that laser CVD films contain hydrogen that effectively saturates the dangling bonds. We have not evaluated the H content so far but we plan to measure it shortly by the hydrogen evolution technique and by infrared spectroscopy.

Optical absorption, particularly in the region of the fundamental gap, gives some interesting results about the "optical" gap and the density of states in the gap.[27] Figure 14 shows the absorptivity, α, as a function of the incident photon energy, $h\nu$, for some of our a-Si:H films. These measurements were made with a Carey Model 17D spectrometer. We have also included for reference data for a-Si (without H) and crystalline silicon.[27]

The attenuation of the reflectance maxima and minima during deposition also can be exploited to yield information about the optical absorptivity of the films. Figure 15 shows a fit to the envelope of the reflectance versus time curve in Figure 10. The value for n is a literature value;[23] α was selected to give a reasonable fit and is within the range of reported values[23] for CVD a-Si and agrees well with the data presented in Figure 14.

The fact that α for a-Si:H is higher than α for crystalline Si in the region around 2 eV photon energy explains why this material is attractive for low cost solar cells. A 1 μm a-Si:H film is equivalent to a 50 μm c-Si film. Even though α of pure a-Si is higher than α of a-Si:H, solar cells made of pure a-Si have poor conversion efficiencies. This is a result of the large concentration of defects in a-Si in the absence of hydrogen. From the α measurements one can deduce an "optical" gap, E_o, using Tauc's expression,[27,28] $(\alpha h\nu)^{1/2} = (h\nu - E_o)$. We find for our films $E_o \approx 1.8$ eV, which is the same order of magnitude as E_o of films of a-Si:H produced by other methods.[5,6] Hydrogen affects the "optical" gap; as one goes from a CVD a-Si film ([H] ~ 0 %) to a high H content glow-discharge a-Si:H film ([H] ~ 30 at. %), E_o changes from 1.45 eV to 2.0 eV.[4] One can understand the increase of E_o with H content as caused by the admixture of the stronger Si-H bonds (~ 3.06 eV) to the Si matrix (Si-Si bond energy is ~ 1.94 eV).

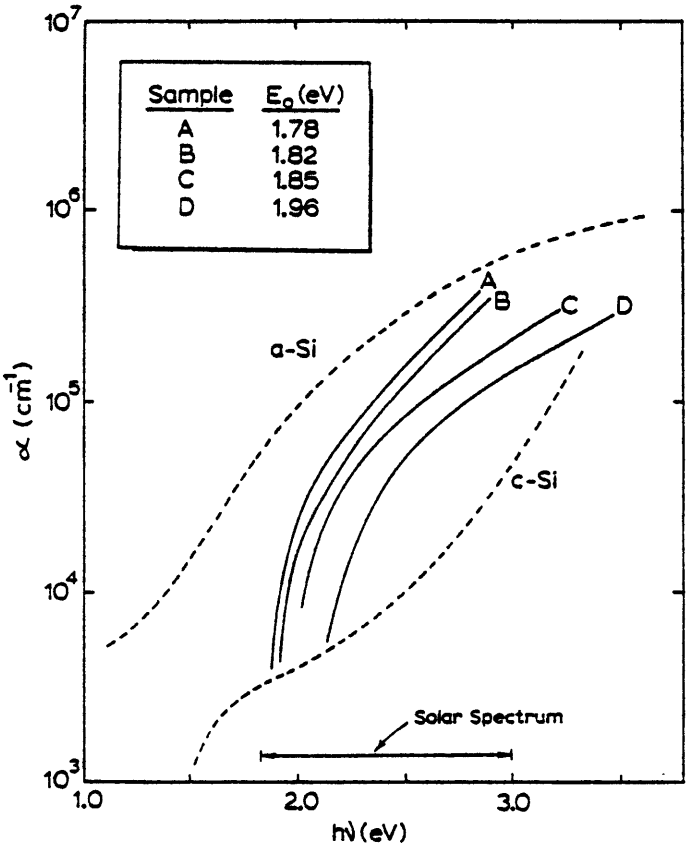

Figure 14. Optical absorption coefficient versus photon energy for several laser CVD a-Si:H films. Also shown are reference data for crystalline silicon and unhydrogenated a-Si from Reference 25.

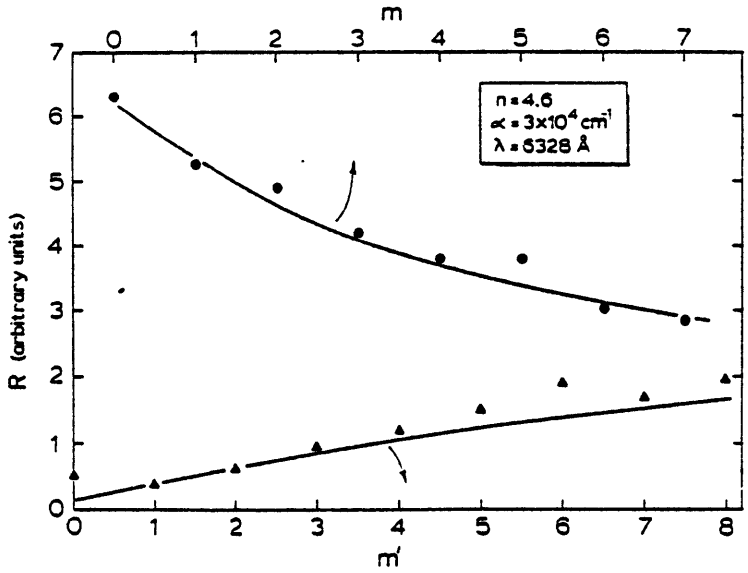

Figure 15. Fit to the envelope of the reflected intensity data of Figure 10. Integers m and m' refer to the order of the maxima and minima, respectively, and are proportional to thickness.

Assuming this relation, we can estimate that our films contain ~ 20 at % hydrogen. Obviously, this has to be checked by direct measurement of hydrogen content.

Conductivity (σ) versus temperature (T) measurements have been made on some films. Figure 16 presents an Arrhenius plot of σ versus 1/T for a film made at T_s = 290°C. The sandwich configuration shown in Figure 17 was used. An activation energy of ~ 0.8 eV is deduced from the high temperature region, which means that the mobility gap is larger than 1.6 eV. This is in good agreement with the "optical" gap of ~ 1.8 eV. However, this measurement presents a problem because the film was very thin (~ 1000 Å). Usually, to prevent contact problems and to ensure bulk conductivity measurements, films of 1 to 2 μm thick are required.[4] The curve in Figure 16 may contain some error but it is expected that the true value of σ is very close to that shown.

V. PROCESS STABILITY

Efforts to completly characterize electrical and optical properties of the laser CVD films have been hampered by an inability to produce consistently films thick enough for these characterizations. This problem is the result of an instability in the deposition process such that with no apparent change in deposition parameters (flow rate, laser power, substrate temperature and cell pressure) the reaction product abruptly changes from film to powder. Resolution of the problem has caused us to conside thermodynamic and kinetics issues and the stability of the CO_2 laser energy source.

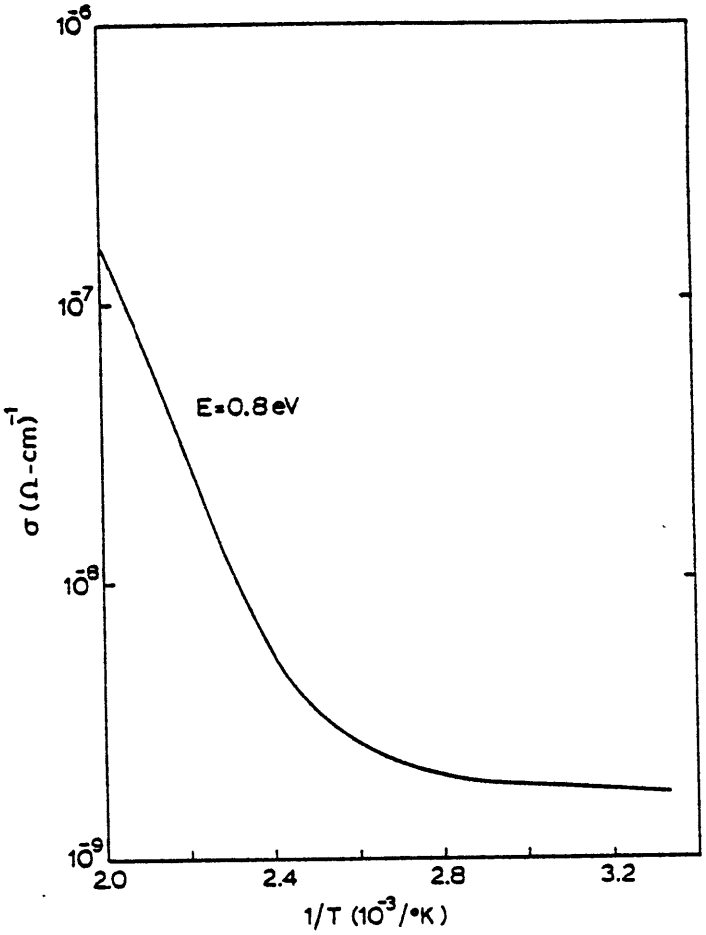

Figure 16. Electrical conductivity versus 1/T for a laser CVD a-Si:H film deposited at a substrate temperature of 290°C with 60 watts of laser power.

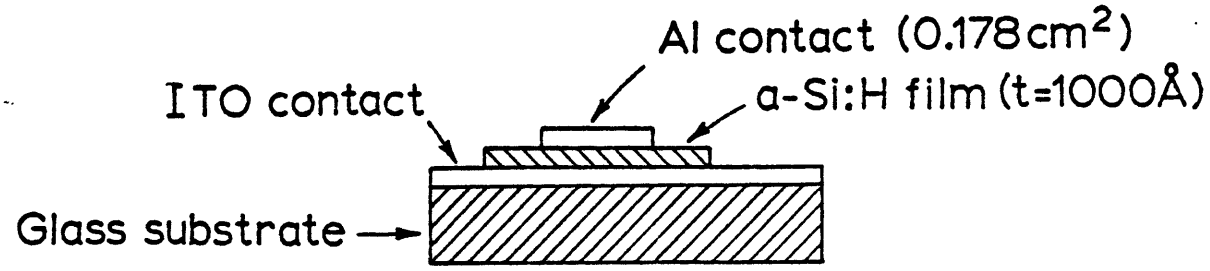

Figure 17. Electrical conductivity sample configuration.

Silane is unstable at all temperatures and thermodynamically it matters little whether the reaction product is film or powder. Film deposition depends on the system being in a condition where heterogeneous nucleation on a substrate is kinetically favored over homogeneous nucleation in the gas phase. The tendency for homogeneous nucleation in the gas phase can be reduced by decreasing the gas pressure, thereby reducing the number of collisions between gas molecules, or by reducing the supersaturation. Lowering the gas pressure narrows the absorption line, causing decoupling of the gas and the laser. Thus this approach cannot be used to stabilize the CVD process beyond a certain point. Alternatively, the nucleation rate can be controlled by reducing the thermodynamic driving force for the reaction. Figure 18 shows the equilibrium hydrogen to silane ratio versus total

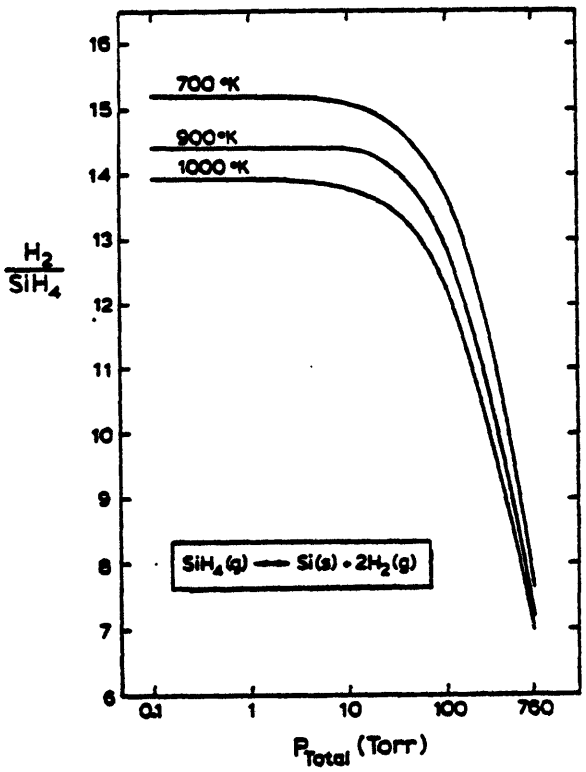

Figure 18. Equilibrium hydrogen to silane ratio versus total pressure and temperature for the pyrolysis of silane.

pressure for the pyrolysis of silane. In the powder process the supersaturation can be controlled by controlling the total pressure because total pressures are around 1 atm. Manipulation of system pressure allows control over the nucleation rate and consequently over the final particle size. However, the supersaturation is independent of P_T for the pressure range used for the CVD process. Thus supersaturaton is controlled by the H_2:SiH_4 ratio.

Flowing gas experiments were carried out with a H_2:SiH_4 ratio up to 10:1 to reduce the supersaturation. At present the gas flow system prohibits higher H_2:SiH_4 ratios at low enough overall flow rates to be useful. Instead of becoming more stable, the system became more unstable. This is easily understood in terms of pressure broadening effect. The amount of hydrogen was not sufficient, as evident from Figure 18 to reduce the supersaturation significantly, but it was sufficient to increase the silane absorptivity significantly through Lorentz broadening, as shown in Figure 2. The net result is that, without reducing the driving force for reaction appreciably, the rate of energy transfer to the gas was increased, thereby increasing the instability. The same effect was observed for mixtures of He and SiH_4, where one would not expect thermodynamic effects. Christensen and Lakin[8] observed similar effects for silane diluted with Ar, although argon is not expected to be as effective in pressure broadening as lighter He or H_2 molecules.[14] An obvious approach to this problem is to alter the gas flow system to allow higher H_2:SiH_4 ratios. More subtle approaches include using chlorosilanes as the silicon source, or use of HCl as the buffer gas rather than H_2.

Recently, an instability was discovered in the laser used for the deposition experiments that could account for the transition in the reaction product. At low power levels the laser output hops between the P20 and P18 lines. This was verified by means of a spectrum analyzer.* The absorption upon which energy transfer depends is extremely wavelength sensitive. The line hopping is equivalent to turning the beam on and off at random, with corresponding expansion and collapse of the gas in the irradiated volume, as described in connection with Figure 6. Resulting nonuniformities in gas composition could account for the abrupt changes in reaction product. The most satisfactory way to deal with this problem is to use a grating-tuned CO_2 laser to ensure P(20) output. We have such a laser on order.

VI. SUMMARY

By means of CO_2 laser-induced pyrolysis of silane gas we have deposited amorphous silicon onto a variety of substrates. Amorphous silicon deposition rates of up to 160 Å/min have been measured in real time (higher rates have been achieved) at substrate temperatures too low (250-350°C) to cause normal pyrolysis of silane. Preliminary measurements of ESR, optical absorptivity and electrical conductivity show that the films produced by this process have properties comparable to the best amorphous Si films produced by glow-discharge techniques. This suggests a high hydrogen content that is the result of the low substrate temperature.

* Optical Engineering Model 16-A

The laser CVD process offers many advantages over conventional pyrolysis techniques. In particular problems of contamination are reduced through the use of a cold-walled reactor and low cost, low temperature substrate materials can be used with pyrolysis reactions that occur only at high temperatures. While only silicon chemistries have been investigated so far there are no fundamental reasons why the process cannot be applied to other systems.

VI. REFERENCES

1. J. S. Haggerty, "Sinterable Powders from Laser Driven Reactions", Energy Laboratory Report MIT-EL 82-002, Massachusetts Institute of Technology, Cambridge, MA (1981).

2. J. C. Knights and G. Lucovsky, "Hydrogen in Amorphous Semiconductors", CRC Critical Reviews in Solid State and Materials Science, 9, 211-83 (1980).

3. D. E. Carlson, "Recent Developments in Amorphous Silicon Solar Cells", Sol. En. Mat., 3, 503-18 (1980); Y. Hamokawa, "Recent Progress of the Amorphous Silicon Solar Cells and Their Technology", Proc. 9th Int. Conf. on Amorphous and Liquid Semiconductors, eds. B. K. Chaknaverty an D. Kaplan, J. de Physique, C4, 1131-42 (1981).

4. H. Fritzche, "Characterization of Glow-Discharge Deposited a-Si:H", Sol. En. Mat., 3, 447-501 (1980).

5. W. Paul and D. Anderson, "Properties of Amorphous Hydrogenated Silicon, with Special Emphasis on Preparation by Sputtering", Sol. En. Mat., 5, 229-316 (1981).

6. M. Hirose, "Physical Properties of Amorphous CVD Silicon", Proc. 9th Int. Conf. on Amorphous and Liquid Semiconductors, eds. B. K. Chakraverty and D. Kaplan, J. de Physique, C4, 705-14 (1981).

7. C. W. White and P. S. Peercy, eds., Laser and Electron Beam Processing of Materials, Academic Press, New York (1980).

8. C. P. Christensen and K. M. Lakin, "Chemical Vapor Deposition of Silicon Using a Laser", Appl. Phys. Lett., 32, 254-5 (1978).

9. V. Baranauskas, C. I. Z. Mammana, R. E. Klinger and J. E. Greene, "Laser-Induced Chemical Vapor Deposition of Polycrystalline Si from $SiCl_4$", Appl. Phys. Lett., 36, 930-2 (1980).

10. S. D. Allen, "Laser Chemical Vapor Deposition: A Technique for Selective Area Deposition", J. Appl. Phys., 52, 6501-5 (1981).

11. R. Bilenchi and M. Musci, "Laser-Enhanced Chemical Vapor Deposition of Silicon", Proc. 8th Int. Conf. on Chemical Vapor Deposition, Electrochemical Society, 275-83 (1981).

12. P. K. Boyer, G. A. Roche, W. H. Ritchie and G. J. Collins, "Laser Induced Chemical Vapor Deposition of SiO_2", Appl. Phys. Lett., 40, 716-9 (1982).

13. T. F. Deutsch, D. J. Ehrlich and R. M. Osgood, Jr., "Laser Photodeposition of Metal Films with Microscopic Features", Appl. Phys. Lett., 35, 175-7 (1979).

14. A. C. G. Mitchell and M. W. Zemansky, Resonance Radiation and Excited Atoms, Cambridge University Press, Cambridge (1961).

15. J. W. C. Johns and W. A. Kreiner, "Measurement and Analysis of the ν_4 Band in Silane", J. Mol. Spec., 60, 400-11 (1976).

16. H. Okabe, Photochemistry of Small Molecules, Wiley, New York (1978).

17. T. F. Deutsch, "Infrared Laser Photochemistry of Silane", J. Chem. Phys., 70, 1187-92 (1979).

18. B. A. Scott, R. M. Plecenik and E. E. Simonyi, "Kinetics and Mechanism of Amorphous Hydrogenated Silicon Growth by Homogeneous Chemical Vapor Deposition", Appl. Phys. Lett., 39, 73-5 (1981).

19. K. H. Sladek, "The Role of Homogeneous Reactions in Chemical Vapor Deposition", J. Electrochem. Soc.: Sol. St. Sci., 118, 654-7 (1971).

20. H. Niki and G. J. Mains, "The $^3P_1$ Mercury Photosensitized Decomposition of Monosilane", J. Phys. Chem., 68, 304-9 (1964).

21. S. K. Friedlander, Smoke, Dust and Haze, Wiley, New York (1977).

22. W. Kern and G. L. Schnable, "Low Pressure Chemical Vapor Deposition for Very Large Scale Integration Processing", IEEE Trans. on Electronic Devices, ED-26, 647-57 (1979).

23. D. C. Booth, D. D. Allred and B. O. Seraphin, "Stabilized CVD Amorphous Silicon for High Temperature Photo-Thermal Solar Energy Conversion", Sol. En. Mat., 2, (1979).

24. J. T. Hilman, "Optical and Electronic Properties of Hydrogenated Amorphous Silicon Films Produced by Laser Enhanced CVD", B. S. Thesis, June 1982.

25. J. Bloem and L. J. Giling, "Mechanisms of the Chemical Vapor Deposition of Silicon", Current Topics in Materials Science, ed. E. Kaldis, 1, 147-342 (1978).

26. D. Adler, "Defects in Amorphous Chalcogenides and Silicon", Proc. 9th Int. Conf. on Amorphous and Liquid Semiconductors, eds. B. K. Chakraverty and D. Kaplan, J. de Physique, C4, 14 (1981).

27. N. F. Mott and E. A. Davis, Electronic Processes in Non-Crystalline Materials, 2nd Ed., Clarendon Press (1979).

28. J. Tauc, "Optical Properties of Non-Crystalline Solids", Optical Properties of Solids, ed. F. Abeles, North-Holland, Amsterdam (1970), pp. 277-313; C. D. Cody et al., "Optical Characterization of Amorphous Silicon Hydride Films", Solar Cells, 2, 227-43 (1980).